The characteristics of the two-component grout on the stress-state in segmental lining

The mechanical characteristics of two-component grout used in segmental lining

Pierpaolo Oreste[1], Giovanni Spagnoli[2]*

[1] Department of Environment, Land and Infrastructure Engineering, Politecnico di Torino, Corso Duca Degli Abruzzi 24, 10129 Torino, Italy; *pierpaolo.oreste@polito.it* ORCID: 0000-0001-8227-9807

[2] DMT GmbH & Co. KG, Am TÜV 1, 45307 Essen, Germany, *giovanni.spagnoli@dmt-group.com* ORCID: 0000-0002-1866-4345 (CORRESPONDING AUTHOR)

Abstract

In this work, the effective influence of the mechanical characteristics of the filling material on the safety factors of the support system is analyzed. Through an extensive parametric analysis, developed by adopting proven analytical methods, on 243 different cases of tunnels excavated using a TBM in a soil mass, at different depths and with different excavation radii, it was possible to identify the conditions in which the safety factors can be effectively low. In all these cases, therefore, it is necessary to intervene on the mechanical characteristics of the filling material, requiring elastic modules and strengths such as to guarantee higher values of the safety factors, avoiding risks on the possible failure of the concrete that makes up the segmental lining and of the same filling material that connects the support system to the tunnel wall.

Key words: two-component grout; filling material; segmental lining; Tunnel Boring Machine (TBM); convergence-confinement method; Einstein and Schwartz method; unconfined compressive strength.

Abbreviations and nomenclature

UCS	Unconfined compressive strength
UCS_{sl}	Unconfined compressive strength for concrete
UCS_{fm}	Unconfined compressive strength for the filling material
c	Cohesion of the ground
C^*	Compressibility ratio of the support system
E	Elastic modulus of the ground
E_{fm}	Elastic modulus of the filling material
E_{sl}	Elastic modulus of the segmental lining (concrete)
F^*	Flexibility ratio of the support system
k_{sys}	Stiffness of the support system
k_{sl}	Radial stiffness of the segmental lining
K_0	Lateral earth pressure at rest in the ground
M_{max}	Maximum moment that develops in the support system
N_{crown}	Normal force at the center of the cap
$N_{sidewall}$	Normal force at the sidewall
p	Pressure inside the tunnel acting on the walls
p_{eq}	Final entity of the loads acting on the support system
p_0	Hydrostatic initial stress state (undisturbed)

R_{pl} Plastic radius of the tunnel

u_{eq} Final entity of the tunnel wall displacement

u_0 Displacement of the tunnel wall when the support system is installed

R Tunnel radius

t_{fm} Thickness of the filling material

t_{sl} Thickness of the segmental lining

z Tunnel depth

ν Poission ratio of the ground

ν_{fm} Poisson's ratio of the filling material

ν_{sl} Poisson's ratio of the concrete constituting the segmental lining

$\sigma_{\vartheta,max}$ Maximum circumferential stresses:

φ Friction angle of the ground

φ_{sl} Friction angle of the concrete

φ_{fm} Friction angle of the filling material

Ψ Dilatancy of the ground

ξ Incremental coefficient that takes into account the transfer of stresses from one ring to the adjacent one

η Coefficient that takes into account the presence of longitudinal joints in segmental lining

Introduction

In mechanized tunnelling excavation, due to the difference between the excavated diameter and the lining external diameter (Do et al., 2013; 2015; Zaheri et al., 2020), a gap is created (e.g. Beghoul and Demagh, 2019; Oggeri et al., 2021;), which must be completely filled in order to lock linings in the designed position and avoid segment movement due to its weight and stresses applied by the surround ground and the shield (Sharghi et al., 2018), to prevent water inflow inside the tunnel increasing the waterproofing, to minimize surface settlements due to the over-excavation generated by the passage of the TBM (Maidl et al., 1995).

The usual mix-design for one m^3 of the two-component grout varies widely and is influenced by the project's specifications, the site's needs, and the availability of equipment. However, it contains cement, bentonite, water, retarder and sodium silicate as an accelerator (e.g. Peila et al., 2011; Di Giulio et al., 2020).

As for the two-component grout, it needs to cure quickly, be stable and to achieve satisfactory short-term compressive strength (Todaro et al., 2022) - normally about 0.5 to 1MPa at 24 hours - in order to control settlements (Sharghi et al., 2018). Besides, its curing environment is confined between the lining and the ground. For that reason, the void grouting cannot be directly observed after the tunnel construction, and therefore it is not simple to simulate its behaviour (Dai et al., 2010), but the quality check can be done only through indirect methods (e.g. Kravitz et al., 2019). The mechanical values of the two-component grout may vary from project to project due to different testing procedures and equipment required to measure strength values (generally Vicat needle and penetrometer for the early curing and compressive strength tests for ages older than 24 hours, see Fig. 1) and a lack of standards regarding the compressive strength assessment (Todaro et al., 2020) creates uncertainty.

Early strength testing are considered to be troublesome because there is no clear norm. Additionally, tests for direct compressive strength can be conducted on cubes or cylinders,

therefore a correlation is required (BS, 1983). Variations in the grout's compressive strength could cause operational and design problems because it is one of the fundamental metrics that demonstrates how well the grout supports the load (Rahmati et al., 2022).

Fig. 1 Vicat needles for early strength (A), penetrometers (B) and a cube for the compressive strength test (C).

While the majority of the literature concerning the two-component grout focuses on the mechanical response of different mix-designs (e.g. Thewes and Budach, 2009; Pelizza et al., 2011; Flores, 2015; Todaro et al., 2021), very little information is available about the interaction with the linings (e.g. Ochmański et al., 2018; Oggeri et al., 2021; 2022; Oreste et al., 2021), or in general about modelling its behaviour, e.g. Bezuijen and Talmon (2003), Oh and Ziegler (2014), Dias and Bezuijen (2015), Shah et al. (2018), Ochmański et al. (2021). The support system made up of the segmental lining and the surrounding filling material has a complex operating mechanism not only due to the presence of joints inside the segmental lining, but also to the evolution of the mechanical parameters of the filling material over time, during the taking period. This evolution leads to varying the overall stiffness of the system and, therefore, the response of the system to the loads transmitted by the soil/rock. In the present study, for simplicity, the filling material has been hypothesized with a single value of its elastic modulus, which must therefore represent the average value that is detected during the stage of its aging.

In this work the effect of the mechanical characteristics of the two-component material on the stress state induced in segmental lining, in the various situations during the excavation of tunnels with a TBM machine is investigated in detail. More specifically, using reliable analytical calculation methods, the stress developing in the segmental lining and in the filling material will be analyzed as the elastic modulus of the latter changes, for different diameters and depths of the tunnel and types of soil.

The results of the developed parametric analysis will be able to indicate the influence of the mechanical characteristics of the filling material on the stress conditions of the segmental lining, in order to determine its physical and mechanical properties required by two-component grout in the tunnel design phase.

The analysis developed in this article using simplified calculation methods allows to estimate the stress state in the segmental lining in order to then proceed to a preliminary sizing of the support system. Further investigations and verifications are, however, required. In fact, a subsequent detailed calculation phase is required with two-dimensional and three-dimensional numerical modeling. This calculation tool requires the construction of the grid of numerical elements and for this reason it is useful, or rather indispensable, to have a preliminary geometric evaluation of the thicknesses of the segmental lining and of the filling material. Finally, the results of the numerical calculation are able to definitively justify the design choices and establish the dimensions of all the components of the support system.

Simplified methods of tunnel segmental lining analysis

A calculation method widely used to analyze the behavior of tunnel supports is the convergence-confinement method, abbreviated as CCM (Oreste, 2003; 2009; Panet and Guenot, 1982; Amberg and Lombardi, 1974). Through this simple method, it is possible to evaluate the final load p_{eq} transmitted by the soil/rock surrounding the tunnel to the adopted supporting system. Two different curves on the internal pressure/radial displacement of the

tunnel wall graph are drawn: the convergence-confinement curve (CCC) and the reaction line of the support system (Fig. 2).

The convergence-confinement method is based on the following fundamental assumptions:

- Circular cavity at a great depth
- Homogeneous mechanical parameters of the ground;
- Hydrostatic type of the undisturbed initial stress p_0 : the vertical stress is equal to the horizontal one.

To obtain a correct evaluation of the load transmitted to the support system, it is necessary to locate the reaction line on the graph and, therefore, define the displacement u_0 of the tunnel wall at the time of installation of the support system. Some calculation procedures are available in the literature to estimate u_0 (e.g. Vlachopoulos and Diederichs, 2009; Spagnoli et al., 2016). In the case of segmental lining installed on the tail of the TBM, i.e. at a certain distance from the tunnel face, a value equal to the displacement corresponding to an internal pressure of $\alpha \cdot p_0$ (α = 0.45-0.50) on the CCC is generally adopted.

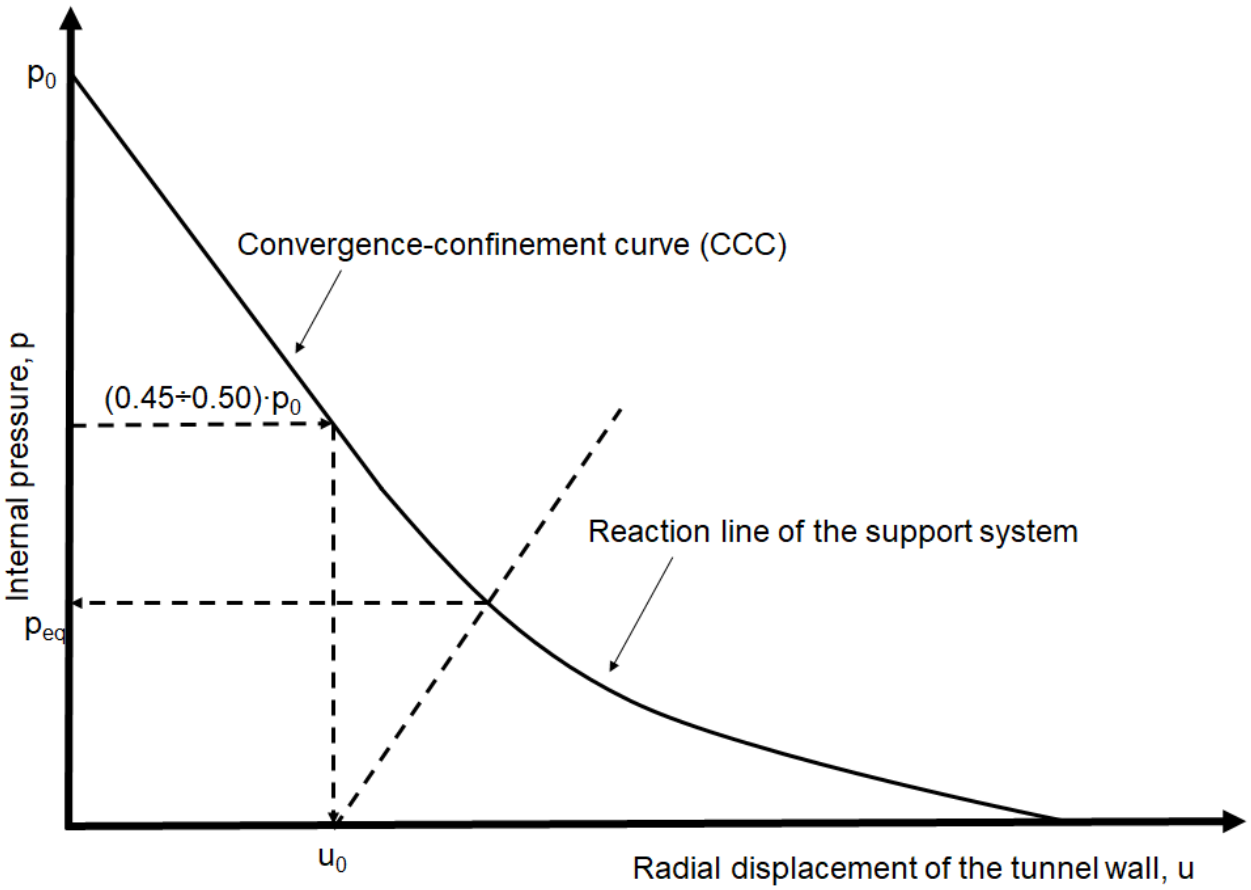

147

148 **Fig. 2. Convergence-confinement method: intersection of the convergence-**
149 **confinement curve with the reaction line of the support system. Key: p: inner pressure**
150 **applied to the tunnel wall; u: radial displacement of the tunnel wall; p_0: in situ vertical**
151 **stress; p_{eq}: final radial load on the support system; u_0: radial displacement of the**
152 **tunnel wall where the support system is installed.**

153 For the case of ideal elasto-plastic behavior of the ground (Oreste, 2009), the convergence-
154 confinement curve can be obtained by evaluating the radial displacement u of the tunnel
155 wall as a function of the internal pressure p, through the following equations:

156
157 For $< \left[p_0 \cdot \left(1 - sin(\varphi)\right) - c \cdot cos(\varphi)\right]$:

$$u = \frac{1+\nu}{E} \cdot \left\{ \left[\frac{R_{pl}^{N_\Psi+1}}{R^{N_\Psi}} \cdot sin(\varphi) + (1-2\cdot\nu) \cdot \left(\frac{R_{pl}^{N_\Psi+1}}{R^{N_\Psi}} - R \right) \right] \cdot \left(p_0 + \frac{c}{tan(\varphi)} \right) - \right.$$

$$\left. \frac{1+N_\Phi \cdot N_\Psi - \nu \cdot (N_\Psi+1) \cdot (N_\Phi+1)}{(N_\Phi+N_\Psi) \cdot R^{(N_\Phi-1)}} \cdot \left(\frac{R_{pl}^{(N_\Phi+N_\Psi)}}{R^{N_\Psi}} - R^{N_\Phi} \right) \cdot \left(p + \frac{c}{tan(\varphi)} \right) \right\} \quad (1)$$

where R_{pl} is the plastic radius of the tunnel:

$$R_{pl} = R \cdot \left[\frac{\left(p_0 + \frac{c}{tan(\varphi)} \right) \cdot \left(1 - sin(\varphi) \right)}{p + \frac{c}{tan(\varphi)}} \right]^{\frac{1}{(N_\Phi-1)}} \quad (2)$$

$$N_\Phi = \frac{1+sin(\varphi)}{1-sin(\varphi)} \quad (3)$$

$$N_\Psi = \frac{1+sin(\Psi)}{1-sin(\Psi)} \quad (4)$$

R is the tunnel radius, c, φ and Ψ are respectively the cohesion, friction angle and dilatancy of the ground, E and ν are respectively the elastic modulus and the Poission ratio of the ground.

For $p > \left[p_0 \cdot \left(1 - sin(\varphi) \right) - c \cdot cos(\varphi) \right]$:

$$u = \frac{1+\nu}{E} \cdot (p_0 - p) \cdot R \quad (5)$$

As regards the reaction line of the support system, it is necessary to consider the presence of segmental lining and filling material (two-component material) in the space between the segmental lining and the surrounding ground (Fig. 3).

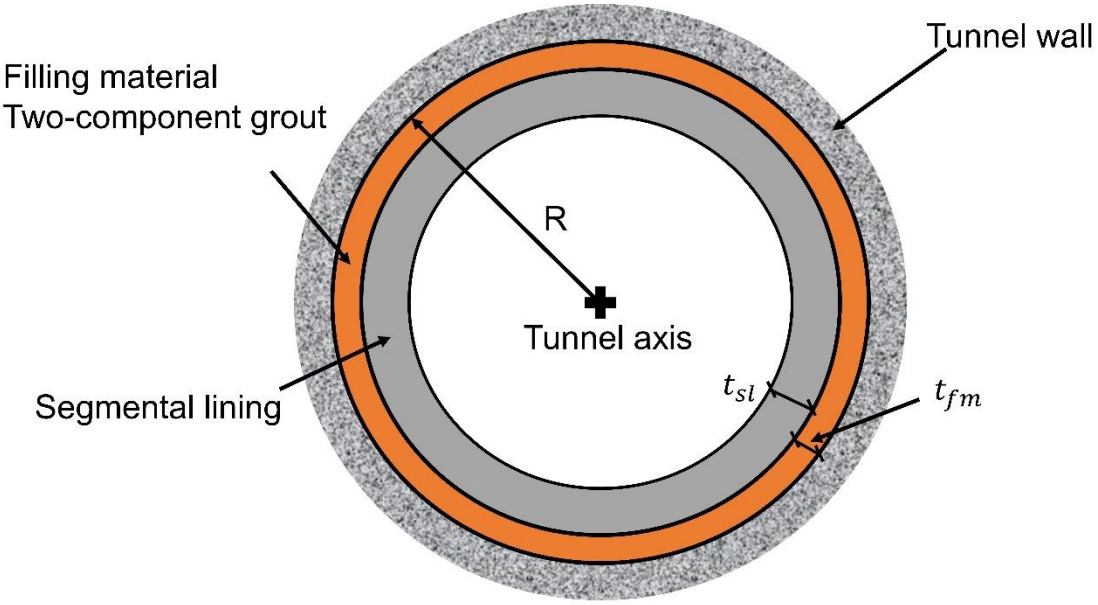

Fig. 3. Cross section of the support system. Key: R: tunnel radius; t_{sl}: thickness of the segmental lining; t_{fm}: thickness of the filling material-not to scale (modified after Oggeri et al. 2021) .

On the basis of what developed by Oreste (2003) it is possible to determine the stiffness of the k_{sys} support system (segmental lining and ring of filling material around it) on the basis of the following equation:

$$k_{sys} = \frac{2 \cdot E_{fm} \cdot (1-\nu_{fm}) \cdot R \cdot \left[\frac{E_{fm}}{(1+\nu_{fm})} + (R-t_{fm}) \cdot k_{sl}\right]}{E_{fm} \cdot (1-2 \cdot \nu_{fm}) \cdot R^2 + (R-t_{fm})^2 \cdot \left[E_{fm} + (1-2 \cdot \nu_{fm}) \cdot (1+\nu_{fm}) \cdot k_{sl} \cdot t_{fm} \cdot \left(1 + \frac{R}{(R-t_{fm})}\right)\right]} - \frac{E_{fm}}{(1+\nu_{fm}) \cdot R} \quad (6)$$

where:

$$k_{sl} = \frac{E_{sl}}{(1+\nu_{sl})} \cdot \frac{(R-t_{fm})^2 - (R-t_{fm}-t_{sl})^2}{(1-2 \cdot \nu_{sl}) \cdot (R-t_{fm})^2 + (R-t_{fm}-t_{sl})^2} \cdot \frac{1}{(R-t_{fm})} \quad (7)$$

E_{fm} and ν_{fm} are respectively the elastic modulus and the Poisson's ratio of the filling material; E_{sl} and ν_{sl} are respectively the elastic modulus and the Poisson's ratio of the segmental lining; t_{fm} and t_{sl} are respectively the thickness of the filling material and segmental lining; k_{sl} is the radial stiffness of the segmental lining.

The stiffness of the support system allows to draw the reaction line of Fig. 2, since it represents the slope of the line on the graph:

$$p = k_{sys} \cdot (u - u_0) \tag{8}$$

In equation 6 it is necessary to introduce the elastic modulus E_{fm} of the two-component material, which shows a variation over time (Oggeri et al., 2021; 2022; Oreste et al., 2021). For this reason, it is necessary to enter an average value representative of the elastic modulus during the period of loading of the support system, taking into account the following parameters that affect this evaluation:

- the downtime of the TBM after the injection of the two-component material;
- the average advancement speed of the TBM after the installation of the segmental lining and the injection of the two-component material.

In the case of a linear elastic behavior of the ground, the convergence-confinement curve becomes a line (eq. 5) and p_{eq} can be obtained from the following simple expression:

$$p_{eq} = \frac{\alpha \cdot p_0}{\frac{E}{(1+\nu) \cdot R \cdot k_{sys}} + 1} \tag{9}$$

k_{sys} it is a very important parameter because it is able to describe the response, in deformation terms, of the support system to the loads applied by the surrounding soil/rock.

For the detailed analysis of support systems, the method of Einstein and Schwartz (1979) can also be used. Through this method it is possible to evaluate the bending moments and the normal forces that develop along the profile of a support system of a circular and deep cavity. The main hypothesis assumed by the authors consists in considering the support system continuously connected to the surrounding ground. An elastic behavior is foreseen both for the ground and for the material constituting the support system. The following equations are able to provide the maximum moment M_{max} that develops in the support system, together with the normal force at the center of the crown N_{crown} and on the sidewalls $N_{sidewall}$ (Einstein and Schwartz, 1979; Guan et al., 2015):

$$M_{max} = (1+\xi) \cdot \frac{p_{eq} \cdot (R - t_{fm})^2 \cdot (1 - K_0)}{(1+K_0) \cdot (1 - a_0^*) + (1 - K_0) \cdot (3 - 6 \cdot a_2^*)} \cdot (1 - 2 \cdot a_2^*) \quad (10)$$

$$N_{crown} = \frac{p_{eq} \cdot R \cdot (1+K_0)}{(1+K_0) \cdot (1 - a_0^*) + (1 - K_0) \cdot (3 - 6 \cdot a_2^*)} \cdot (2 \cdot a_2^* - a_0^*) \quad (11)$$

$$N_{sidewall} = \frac{p_{eq} \cdot R \cdot (1+K_0)}{(1+K_0) \cdot (1 - a_0^*) + (1 - K_0) \cdot (3 - 6 \cdot a_2^*)} \cdot (2 - a_0^* - 2 \cdot a_2^*) \quad (12)$$

where:

$$a_0^* = \frac{C^* \cdot F^* \cdot (1 - \nu)}{C^* + F^* + C^* \cdot F^* \cdot (1 - \nu)} \quad (13)$$

$$a_2^* = \frac{(F^* + 6) \cdot (1 - \nu)}{2 \cdot F^* \cdot (1 - \nu) + 6 \cdot (5 - 6 \cdot \nu)} \quad (14)$$

$$C^* = \frac{E \cdot R \cdot (1 - \nu_{sl}^2)}{\left(E_{fm} + E_{sl} \cdot \frac{t_{sl}}{t_{sl} + t_{fm}}\right) \cdot (t_{fm} + t_{sl}) \cdot (1 - \nu^2)} \quad (15)$$

$$F^* = \eta \cdot \frac{12 \cdot E \cdot (R - t_{fm})^3 \cdot (1 - \nu_{sl}^2)}{E_{sl} \cdot t_{sl}^3 \cdot (1 - \nu^2)} \quad (16)$$

K_0 is the lateral earth pressure at rest in the ground (in the initial undisturbed conditions);

E and ν are respectively the elastic modulus and the Poisson ratio of the ground;

C^* and F^* are compressibility ratio and flexibility ratio of the support system, respectively. In evaluating C^* it was assumed that the average elastic modulus representative of the support system is the average of the values of the segmental lining and the filling material, weighted on the respective thicknesses. As regard F^*, only the contribution from segmental lining is assumed, neglecting the presence of the filling material.

ξ is an incremental coefficient that takes into account the transfer of stresses from one ring to the adjacent one, in correspondence with the longitudinal joints of the segmental lining; a value of 0.45 can be used (Guan et al., 2015). η is a coefficient that takes into account the presence of longitudinal joints in segmental lining, reducing its bending stiffness with respect to a continuous lining; it varies between 0.4 and 0.7, with an intermediate value of 0.55 (Guan et al., 2015).

The simplified analysis of the stress state in the segmental lining (sl) and in the filling material (fm) leads to the following maximum circumferential stresses $\sigma_{\vartheta,max}$:

$$\sigma_{\vartheta,max,sl} = \frac{6 \cdot M_{max}}{t_{sl}^2} + \frac{max(N_{crown};N_{sidewall})}{t_{sl}} \cdot \frac{E_{sl} \cdot t_{sl}}{E_{sl} \cdot t_{sl} + E_{fm} \cdot t_{fm}} \quad (17)$$

$$\sigma_{\vartheta,max,fm} = \frac{max(N_{crown};N_{sidewall})}{t_{fm}} \cdot \frac{E_{fm} \cdot t_{fm}}{E_{sl} \cdot t_{sl} + E_{fm} \cdot t_{fm}} \quad (18)$$

In the definition of the stress state, it is assumed that the bending moment is completely absorbed by the segmental lining alone, since the bending stiffness of the filling material is negligible. The normal force N is distributed, on the other hand, in a proportional way to the normal stiffness, between the segmental lining and the filling material.

In addition to the circumferential stresses obtained by eq. 17 and 18, it is also necessary to consider the presence of radial stresses, which are in both cases equal to p_{eq}.

Once the stress state induced in the two materials is known, it is possible to determine the safety factors in relation to the risk of a possible failure, adopting the Mohr-Coulomb strength criterion:

$$F_{s,sl} = \frac{UCS_{sl} + \frac{1+sin(\varphi_{sl})}{1-sin(\varphi_{sl})} \cdot p_{eq}}{\sigma_{\vartheta,max,sl}} \tag{19}$$

$$F_{s,fm} = \frac{UCS_{fm} + \frac{1+sin(\varphi_{fm})}{1-sin(\varphi_{fm})} \cdot p_{eq}}{\sigma_{\vartheta,max,fm}} \quad \text{if } \sigma_{\vartheta,max,fm} \geq p_{eq} \tag{20a}$$

$$F_{s,fm} = \frac{UCS_{fm} + \frac{1+sin(\varphi_{fm})}{1-sin(\varphi_{fm})} \cdot \sigma_{\vartheta,max,fm}}{p_{eq}} \quad \text{if } \sigma_{\vartheta,max,fm} < p_{eq} \tag{20b}$$

Where UCS and φ are respectively the uniaxial compression strength and the friction angle of the material (concrete for segmental lining or filling material).

The evaluation of the safety factors with regard to the possible failure of the two materials constituting the support system is able to drive the design phase and define the mechanical and geometric characteristics. More specifically, it will be necessary to evaluate:

- the thickness of the segmental lining and the filling material;
- the required average elastic modulus of the two-component material that constitutes the filling material, during the loading phase of the support system.

Results and discussion

To evaluate the stress state induced in the segmental lining and in the filling material in the various cases that may be encountered during the construction of a tunnel using a TBM in a soil mass, a parametric analysis was developed consisting of 243 cases, varying:

- Tunnel radius R: 2, 3.5 and 5 m;
- Tunnel depth z: 25, 100, 175 m;
- Elastic modulus of the filling material E_{fm}: 50, 500 and 1000 MPa;
- Type of ground: soft (E=100 MPa), medium (E =500 MPa) and stiff (E =1000 MPa);
- Lateral earth pressure at rest in the ground K_0: 0.5, 1.0 and 1.50;

The values adopted in the analysis represent the extremes and the central value of the variability ranges of the single parameters, which are typically encountered in the excavation of tunnels with TBM machines. They have been identified through an extensive analysis of real cases of tunnels for which the TBM has been adopted as a means of excavation.

By elastic modulus E_{fm} of the filling material, it is meant the average elastic modulus of the two-component during the loading phase of the support system, that is, in the first phases following its installation in which the Tunnel Boring Machine (TBM) moves forward.

A recurring value of the thickness of the segmental lining (t_{sl}) of 30 cm is adopted in the calculations. The thickness of the filling material was assumed to be 15 cm (t_{fm}). For the elastic modulus of the concrete a value equal to 35 GPa (E_{sl}) was considered. The Poisson ratios used in the calculation were 0.30 (ν), 0.15 (ν_{sl}), 0.09 (ν_{fm}), respectively for the ground, concrete and filling material. The value of the η coefficient in equation 15 was cautiously assumed to be 0.4, i.e. equal to the minimum value of its detected variability interval. The UCS strength for the concrete was assumed to be 40 MPa (UCS_{sl}), while for the filling material a value of 1 MPa (UCS_{fm}) was cautiously adopted, the minimum value among those

detected in the laboratory tests available in the literature. The friction angles of the concrete (φ_{sl}) and of the filling material (φ_{fm}) have been set equal to 40° and 30°, respectively.

The results of the calculation in terms of maximum circumferential stress in the segmental lining ($\sigma_{\vartheta,max,sl}$ of eq. 17) together with the safety factors *FS,sl* and *FS,fm* (eq. 19 and 20), are shown in the following figures. They allow detecting the effects of the influencing parameters, in particular of the two-component filling material, on the induced stress-state of the tunnel segmental lining and of the same filling material.

Figures 4 to 6 show the maximum circumferential stresses in segmental lining ($\sigma_{\vartheta,max,sl}$) as the coefficient K_0 varies for the case of tunnel radius R = 3.5 m, respectively for a depth of 25 m (Fig. 4), 100 m (Fig. 5) and 175 m (Fig. 6). It can be seen how the maximum stresses in concrete always increase as K_0 distances from the unit, reaching significantly larger values for K_0 = 0.5 or K_0 = 1.5. Furthermore, the elastic modulus of the ground E has a significant importance on the maximum stress in the concrete of segmental lining: as the elastic modulus decreases, the stress increases significantly, especially when the elastic modulus is less than 500 MPa. As regards the elastic modulus of the two-component material E_{fm}, its effect on the maximum stress in the concrete is noted, especially when the elastic modulus of the ground E is high and only for E_{fm} <500 MPa. In fact, in all the analyzed cases, there is no difference in the maximum stress as the E_{fm} varies between 500 and 1000 MPa. The depth of the tunnel obviously has effects on the stress state of the segmental lining: as the depth increases, the maximum stress in the segmental lining increases, almost proportional to the depth. The trend of the shown diagrams, however, remains the same at different depths, varying only the value of the stress.

For smaller tunnel radii (R = 2 m) the same considerations seen for R = 3.5 m apply, with the only exception that the growth of the maximum stress is not particularly marked for elastic modules of the ground E below 500 MPa. On the contrary, for R = 5 m, the significant

increase in the maximum stress for E <500 MPa detected in the case of 3.5 m radius is even more pronounced.

Obviously, there is a reduction in the stress state in the segmental lining as the tunnel radius decreases and the opposite for larger radii.

Of particular interest is the analysis of the safety factors of segmental lining with regard to concrete failure. The following figures (Fig. 7-15) show the $FS_{,sl}$ as K_0, E and E_{fm} vary, for the three values of R and the three of z considered in the analysis.

The lowest safety factors $FS_{,sl}$ are obtained for K_0 far from the unit, for E_{fm} greater than 500 MPa and for lower elastic modules of the ground E. When E is low, the effect of E_{fm} on the safety factors of the segmental lining vanishes. Furthermore, for E_{fm}> 500 MPa the influence of the elastic modulus of the two-component material on the safety factor of the segmental lining is never detected. Obviously the $FS_{,sl}$ tend to decrease with the increasing depth and tunnel radius.

The graphs shown can be very useful in the design phase, in order to decide the characteristics of the two-component material to fill the gap between the segmental lining and the tunnel wall and the thicknesses of the segmental lining and the filling material. Only through an evaluation of the safety factors, in fact, it is possible to decide the fundamental parameters of the support system design in order to guarantee a certain distance from risk situations in relation to the possible failure of the concrete.

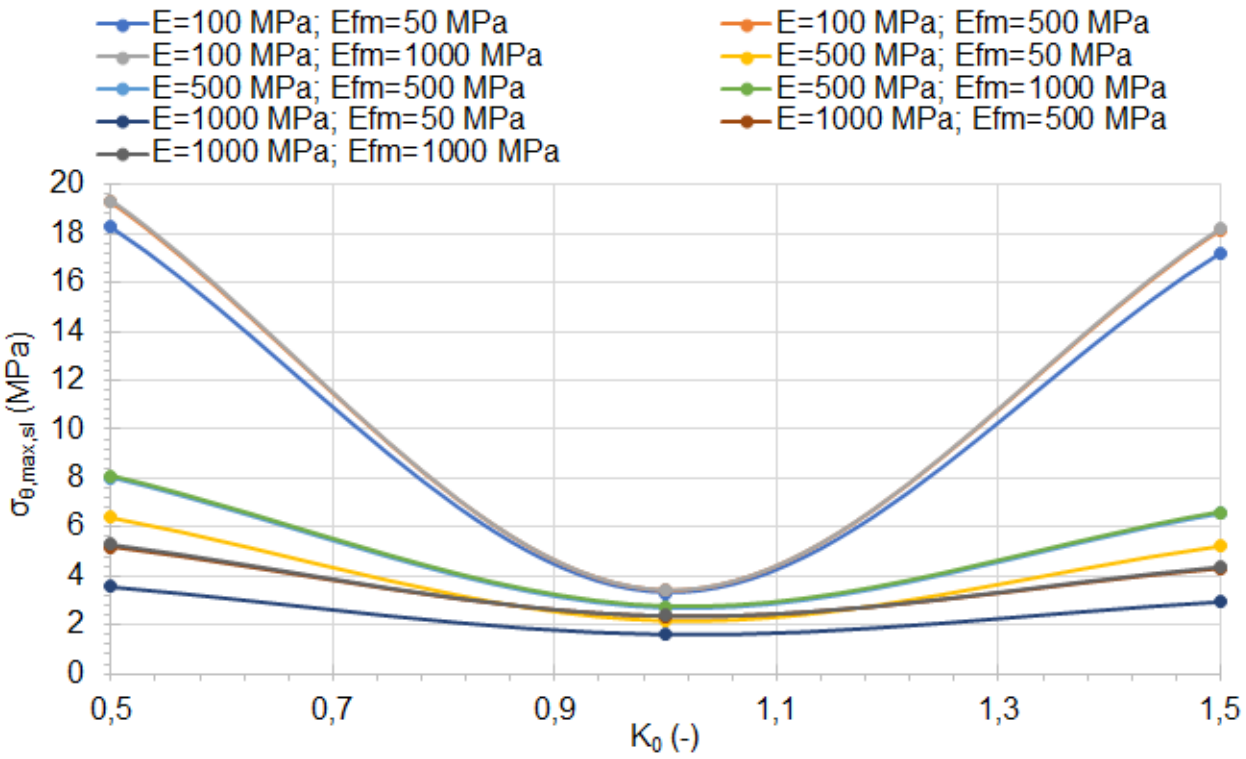

Fig. 4. Maximum circumferential stress ($\sigma_{\vartheta,max,sl}$) in the concrete of the segmental lining, as the coefficient K_0 varies for different values of the elastic modulus of the ground (E) and of the elastic modulus of the filling material (E_{fm}). Case of a tunnel with radius R = 3.5 m and depth z = 25 m.

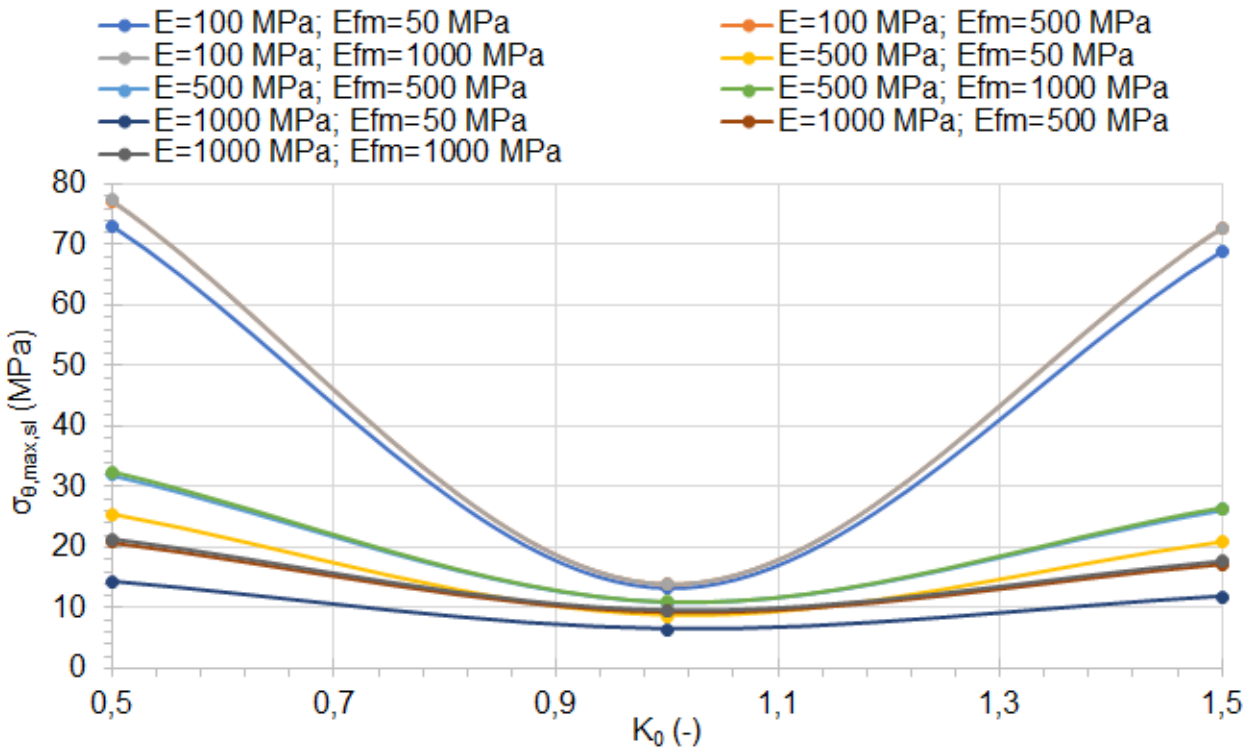

330

331 **Fig. 5. Maximum circumferential stress ($\sigma_{\vartheta,max,sl}$) in the concrete of the segmental**
332 **lining, as the coefficient K_0 varies for different values of the elastic modulus of the**
333 **ground (E) and of the elastic modulus of the filling material (E_{fm}). Case of a tunnel**
334 **with radius R = 3.5 m and depth z = 100 m.**

335

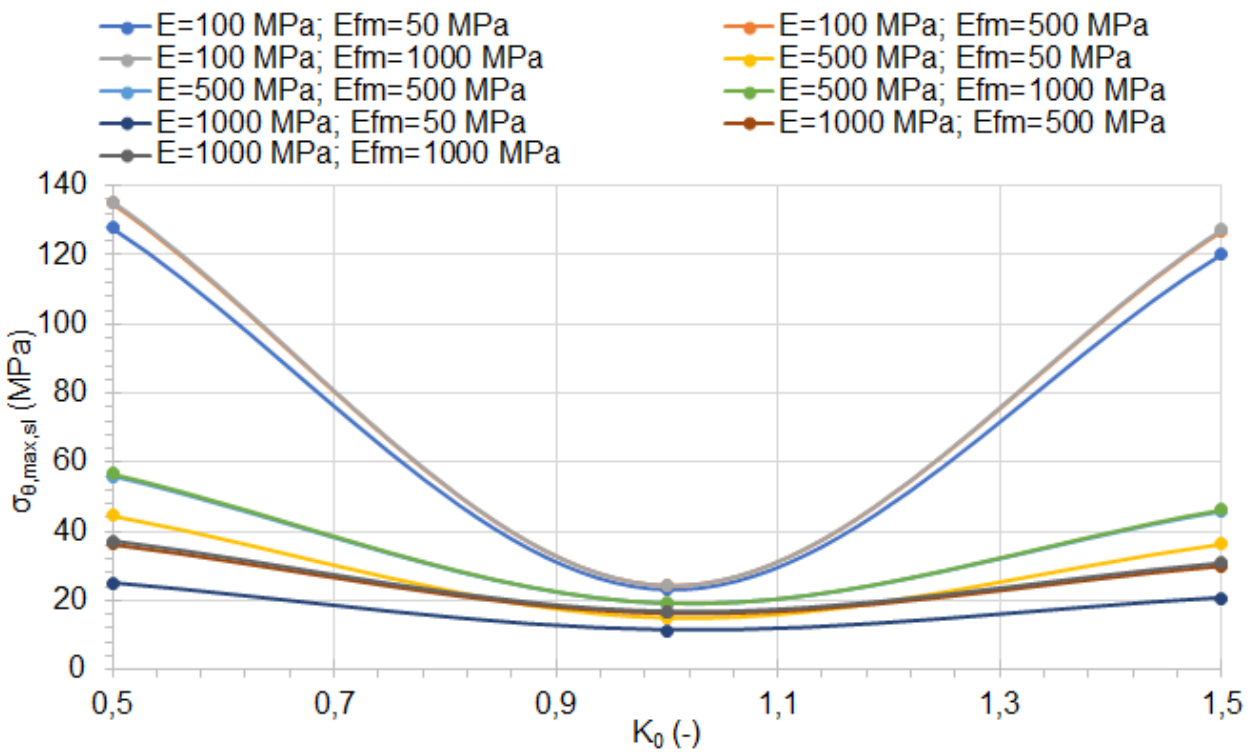

Fig. 6. Maximum circumferential stress ($\sigma_{\vartheta,max,sl}$) in the concrete of the segmental lining, as the coefficient K_0 varies for different values of the elastic modulus of the ground (E) and of the elastic modulus of the filling material (E_{fm}). Case of a tunnel with radius R = 3.5 m and depth z = 175 m.

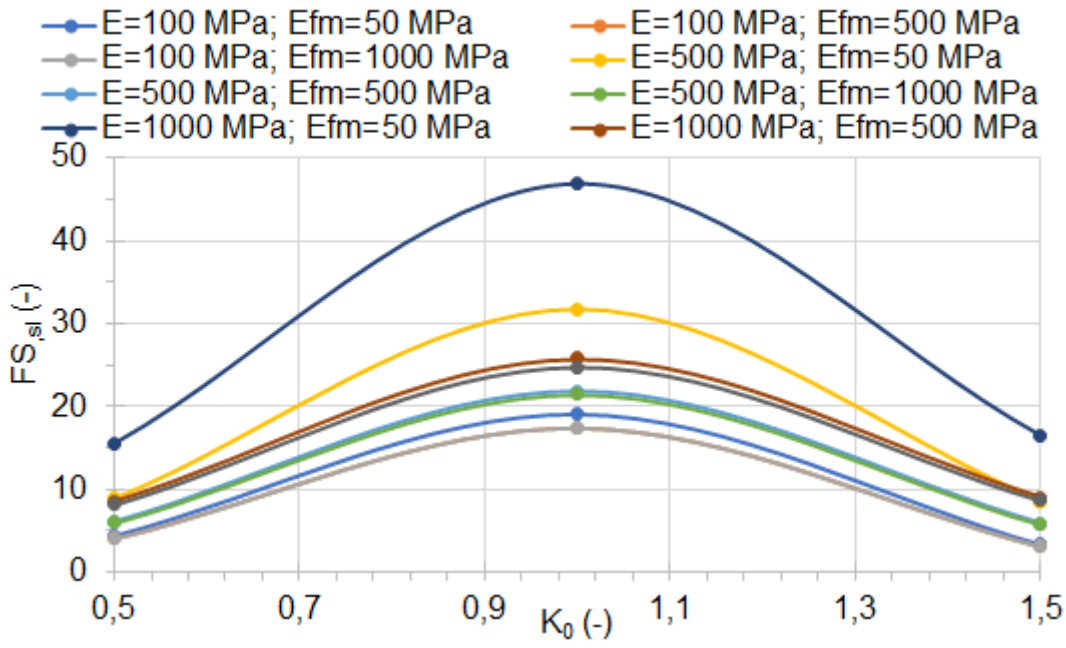

343

344 **Fig. 7. Safety factors in segmental lining (*FS,sl*) as the coefficient K_0 varies for**
345 **different values of the elastic modulus of the ground (E) and of the elastic modulus**
346 **of the filling material (E_{fm}). Case of a tunnel with radius R = 2 m and depth z = 25 m.**

347

348

349

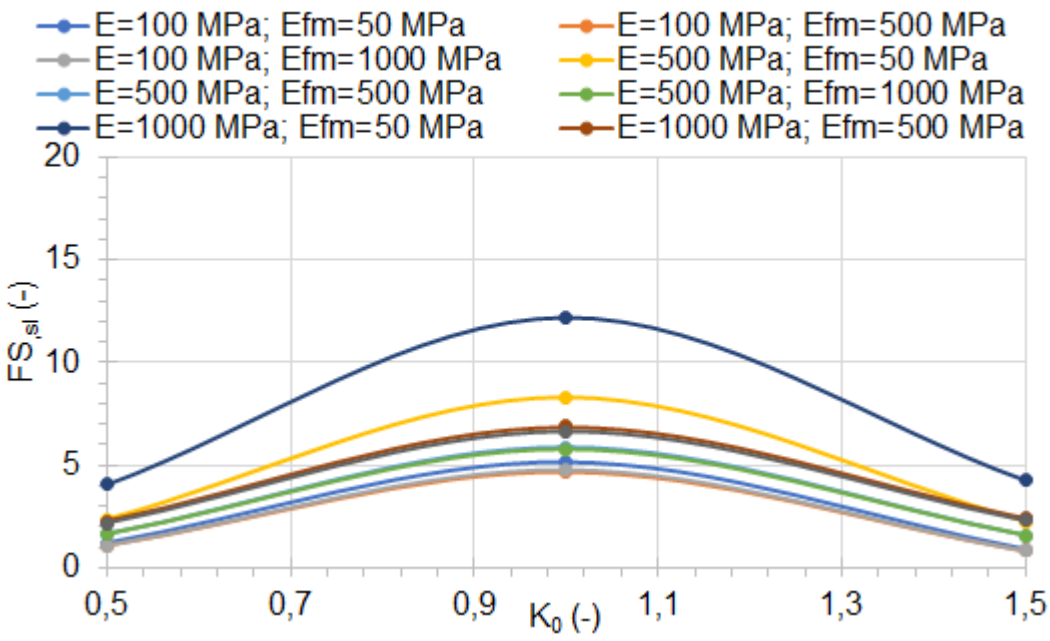

Fig. 8. Safety factors in segmental lining (*FS,sl*) as the coefficient K_0 varies for different values of the elastic modulus of the ground (E) and of the elastic modulus of the filling material (E_{fm}). Case of a tunnel with radius R = 2 m and depth z = 100 m.

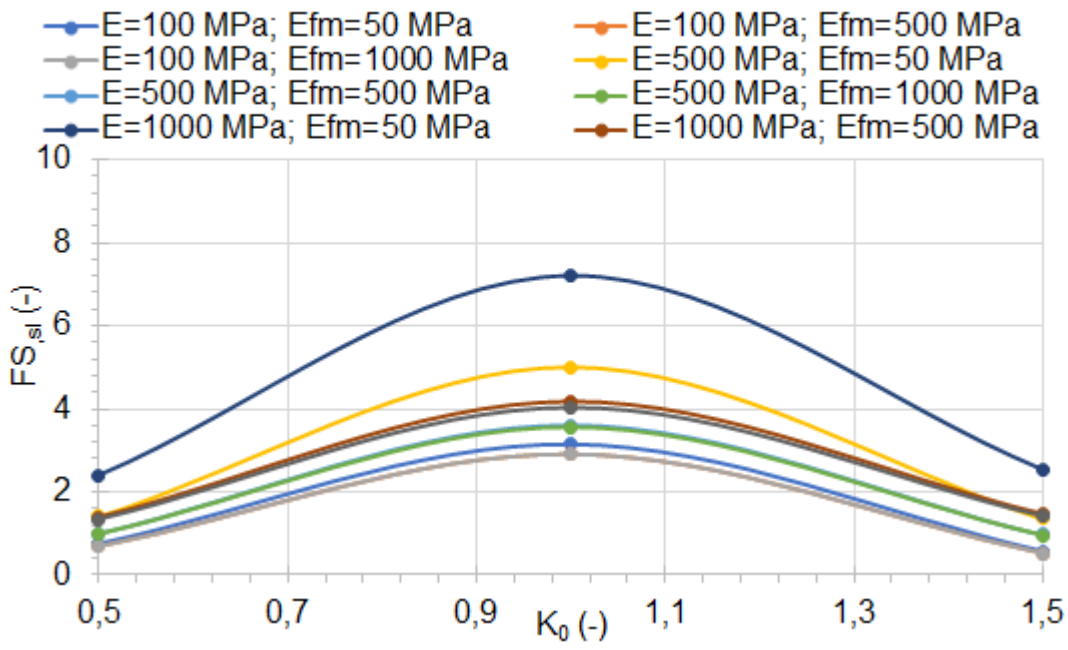

358

359 **Fig. 9. Safety factors in segmental lining (*FS,sl*) as the coefficient K_0 varies for**
360 **different values of the elastic modulus of the ground (E) and of the elastic modulus**
361 **of the filling material (E_{fm}). Case of a tunnel with radius R = 2 m and depth z = 175 m.**

362

363

364

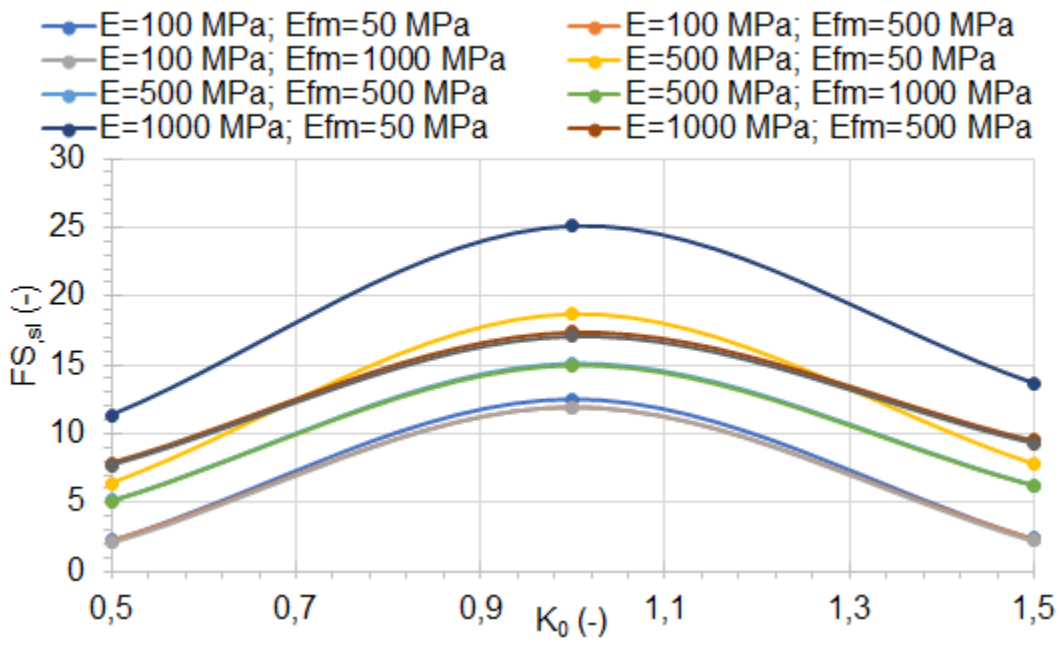

365

366 **Fig. 10. Safety factors in segmental lining (*FS,sl*) as the coefficient K_0 varies for**
367 **different values of the elastic modulus of the ground (E) and of the elastic modulus**
368 **of the filling material (E_{fm}). Case of a tunnel with radius R = 3.5 m and depth z = 25 m.**

369

370

371

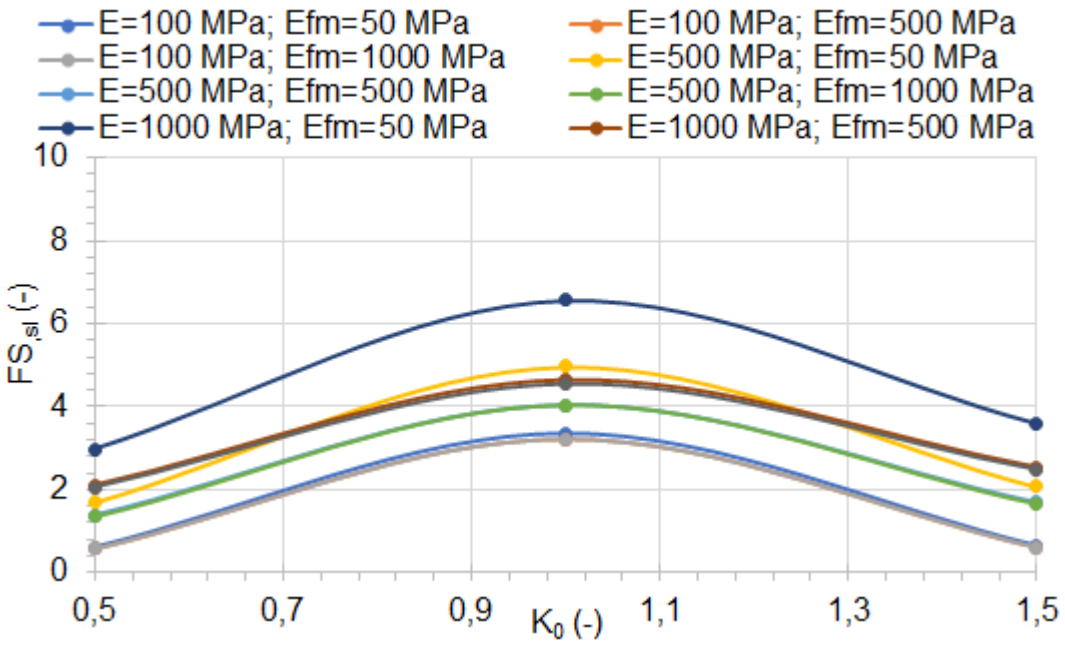

372

373 **Fig. 11. Safety factors in segmental lining (*FS,sl*) as the coefficient K_0 varies for**
374 **different values of the elastic modulus of the ground (E) and of the elastic modulus**
375 **of the filling material (E_{fm}). Case of a tunnel with radius R = 3.5 m and depth z = 100**
376 **m.**

377

378

379

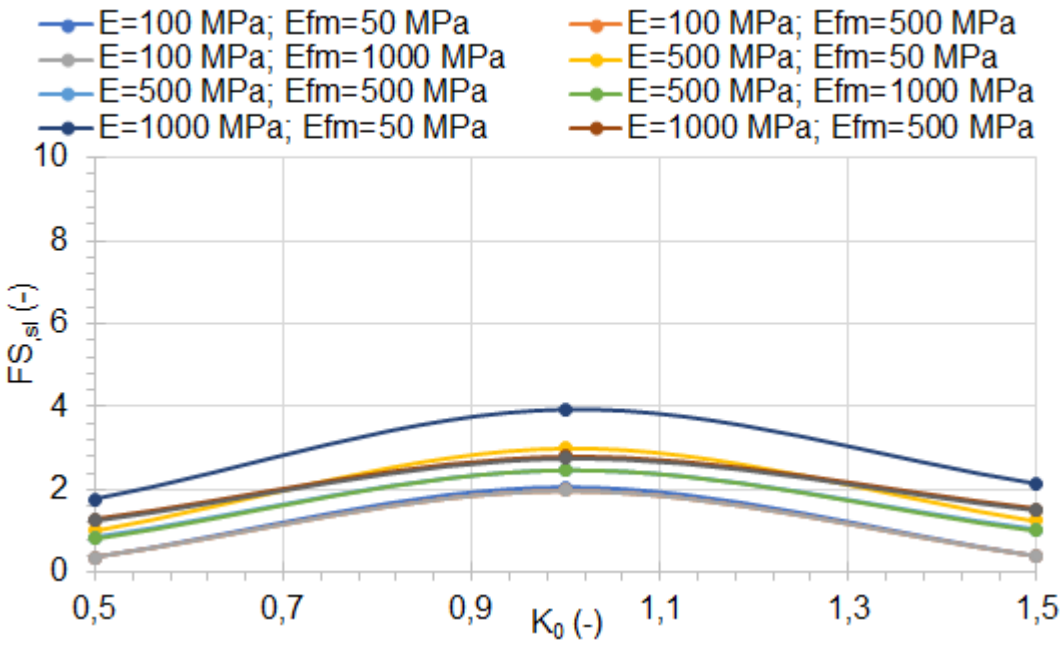

Fig. 12. Safety factors in segmental lining (*FS,sl*) as the coefficient K_0 varies for different values of the elastic modulus of the ground (E) and of the elastic modulus of the filling material (E_{fm}). Case of a tunnel with radius R = 3.5 m and depth z = 175 m.

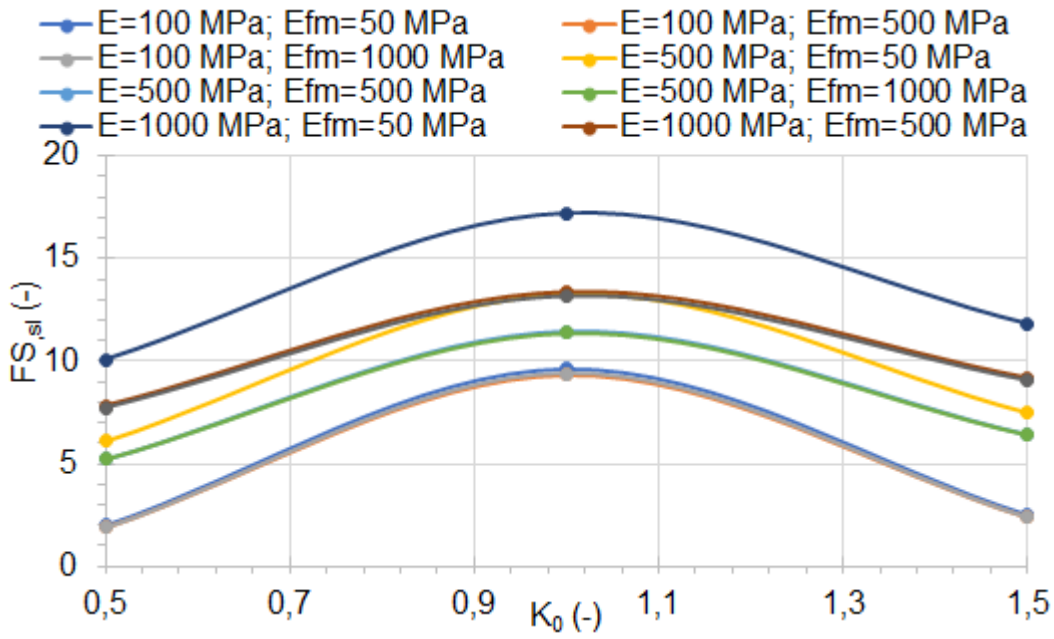

388

389 **Fig. 13. Safety factors in segmental lining (*FS,sl*) as the coefficient K_0 varies for**
390 **different values of the elastic modulus of the ground (E) and of the elastic modulus**
391 **of the filling material (E_{fm}). Case of a tunnel with radius R = 5 m and depth z = 25 m.**

392

393

394

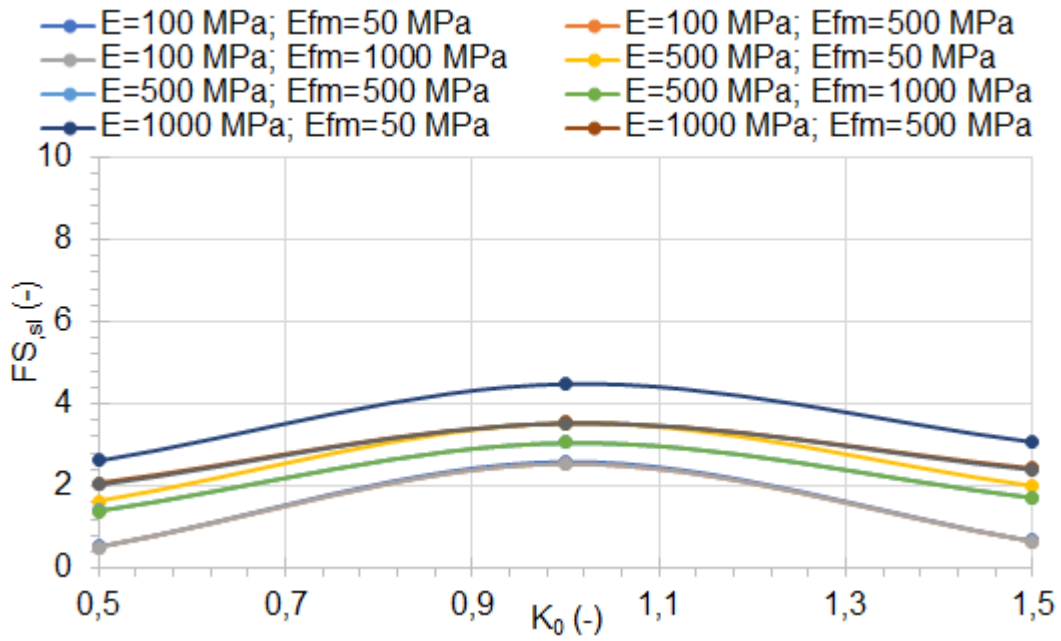

395

396 **Fig. 14. Safety factors in segmental lining (*FS,sl*) as the coefficient K_0 varies for**
397 **different values of the elastic modulus of the ground (E) and of the elastic modulus**
398 **of the filling material (E_{fm}). Case of a tunnel with radius R = 5 m and depth z = 100 m.**

399

400

401

402

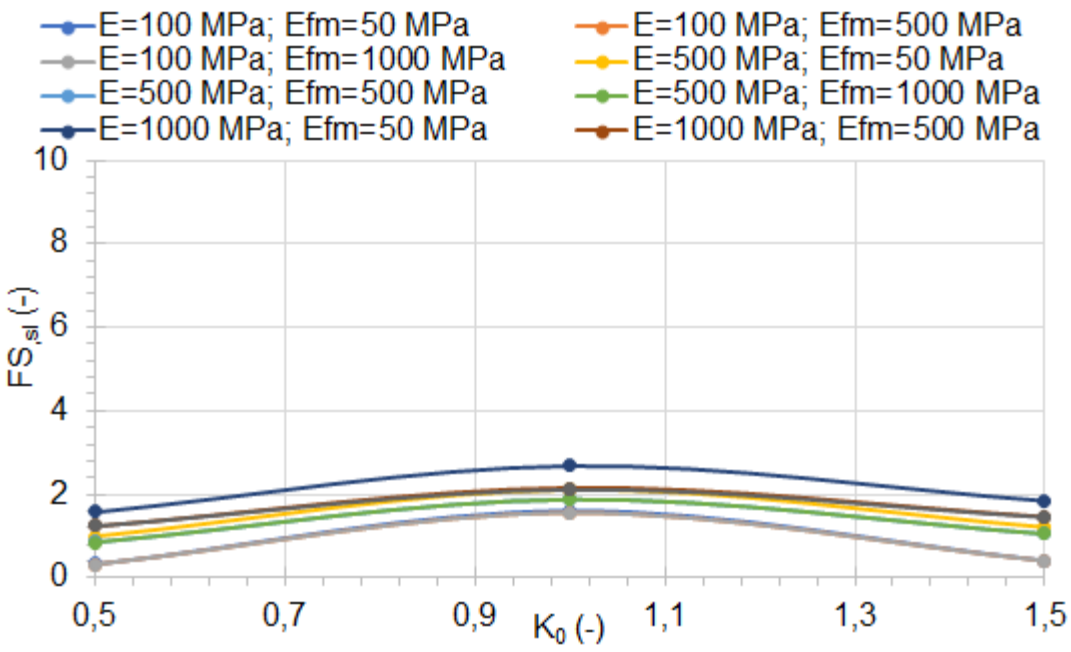

403

404 **Fig. 15. Safety factors in segmental lining (*FS,sl*) as the coefficient K_0 varies for**
405 **different values of the elastic modulus of the ground (E) and of the elastic modulus**
406 **of the filling material (E_{fm}). Case of a tunnel with radius R = 5 m and depth z = 175 m.**

407

408 As for the safety factors of the filling material with regard to failure due to the stress state
409 induced inside it, it can be noted that the coefficient K_0 has no importance: in fact, since the
410 filling material has a negligible bending stiffness, the moments that develop inside it are
411 practically nil; the existing circumferential stresses are due solely to the normal force N.
412 Figures 16-18 show the $FS_{,fm}$ as the depth z varies, for the different values of E and E_{fm}
413 considered in the analysis, for the cases of R = 2 m (Fig. 16), R = 3.5 (Fig. 17) and R = 5 m
414 (Fig. 18).
415 These safety factors were calculated by adopting a precautionary UCS_{fm} strength equal to
416 1 MPa. It is clear that by intervening to increase the UCS_{fm}, an increase in the safety factor
417 and a reduction in the risk of failure of the filling material around the segmental lining can be
418 obtained.

From the analysis of Fig. 16 it can be seen how the $FS_{,fm}$ tends to decrease considerably up to 100-120 m in depth and then stabilize at minimum values. The depth of the tunnel, therefore, plays a fundamental role with regards to the possible risk of failure of the filling material, with all the possible consequences on the infiltration of groundwater into the tunnel and on the consequent possible chemical-physical aggression on the concrete of the segmental lining. The lowest values of the safety factor are obtained in correspondence of a ground with a low elastic modulus E and of a low stiffness of the filling material E_{fm}.

The size of the tunnel has a marginal influence as can be seen with the comparison with Fig.17-18.

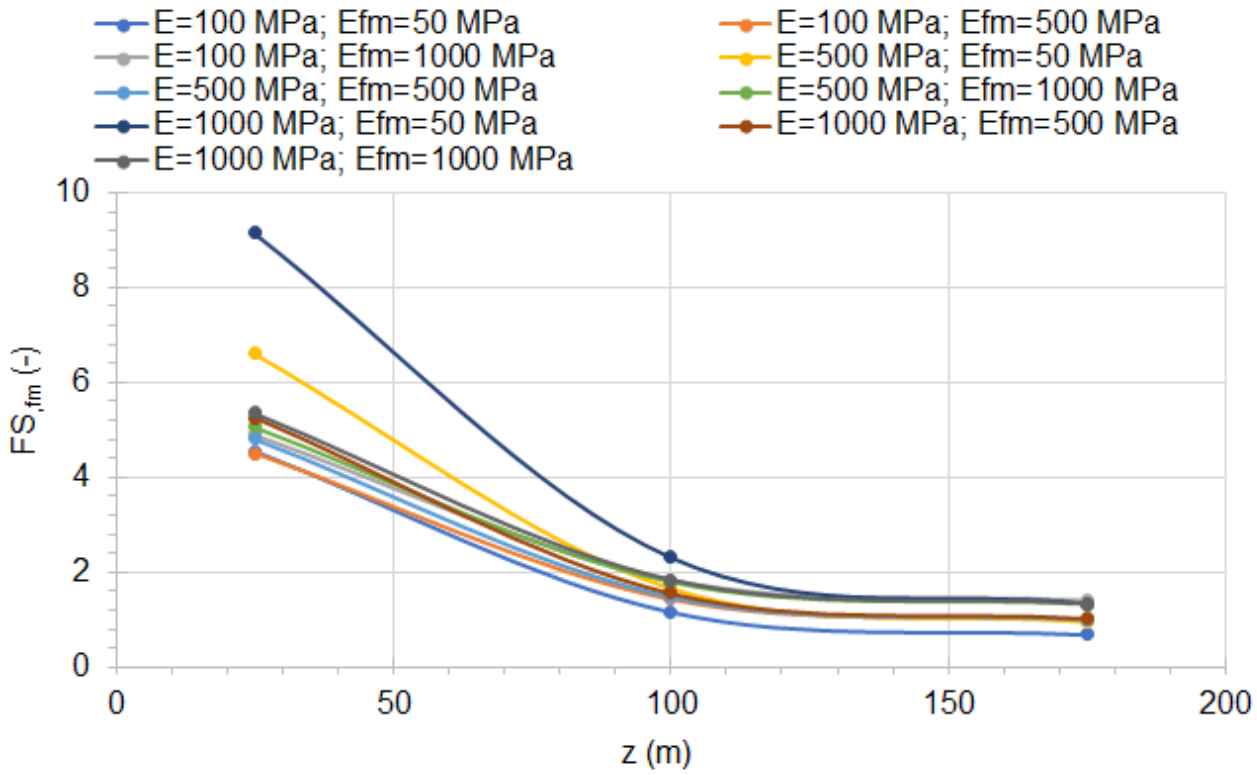

Fig. 16. Safety factors in the filling material ($FS_{,fm}$) as the depth z of the tunnel varies, for different values of the elastic modulus of the ground (E) and of the elastic modulus of the filling material (E_{fm}). Case of a tunnel with radius R = 2 m.

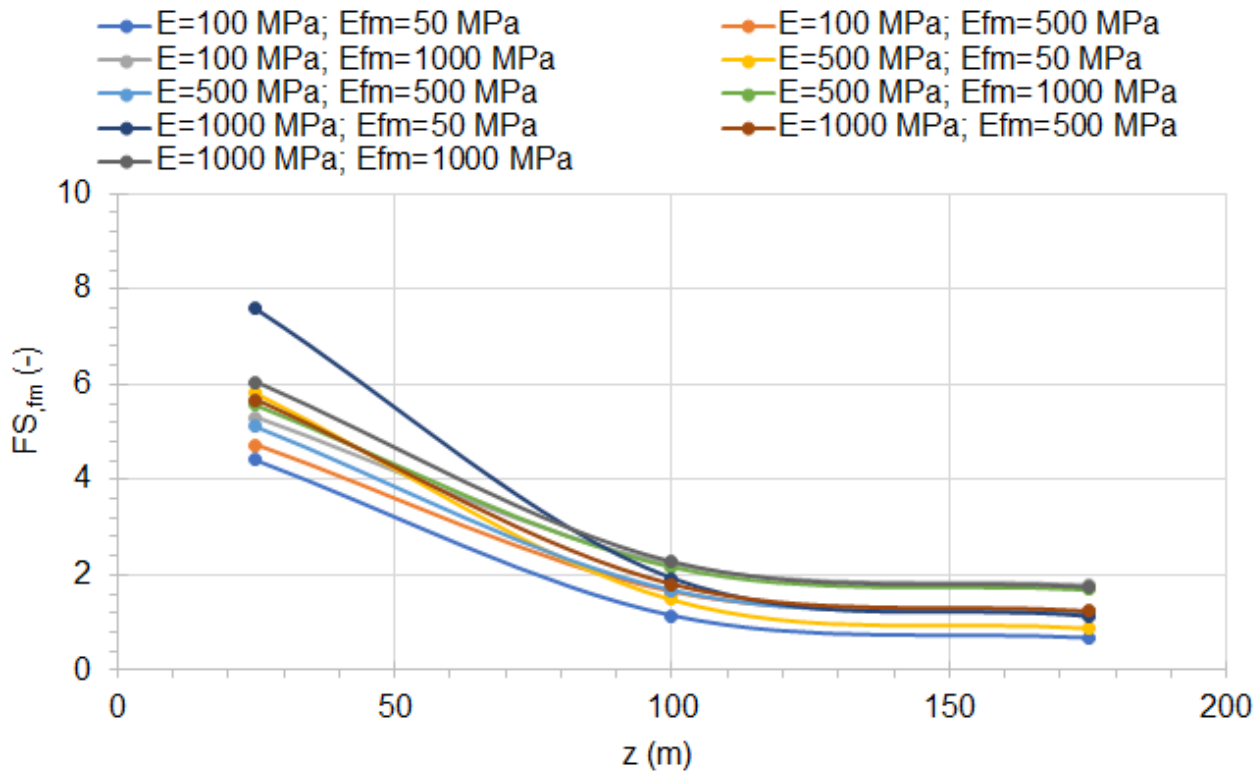

434

435 **Fig. 17. Safety factors in the filling material ($F_{S,fm}$) as the depth z of the tunnel varies,**

436 **for different values of the elastic modulus of the ground (E) and of the elastic modulus**

437 **of the filling material (E_{fm}). Case of a tunnel with radius R = 3.5 m.**

438

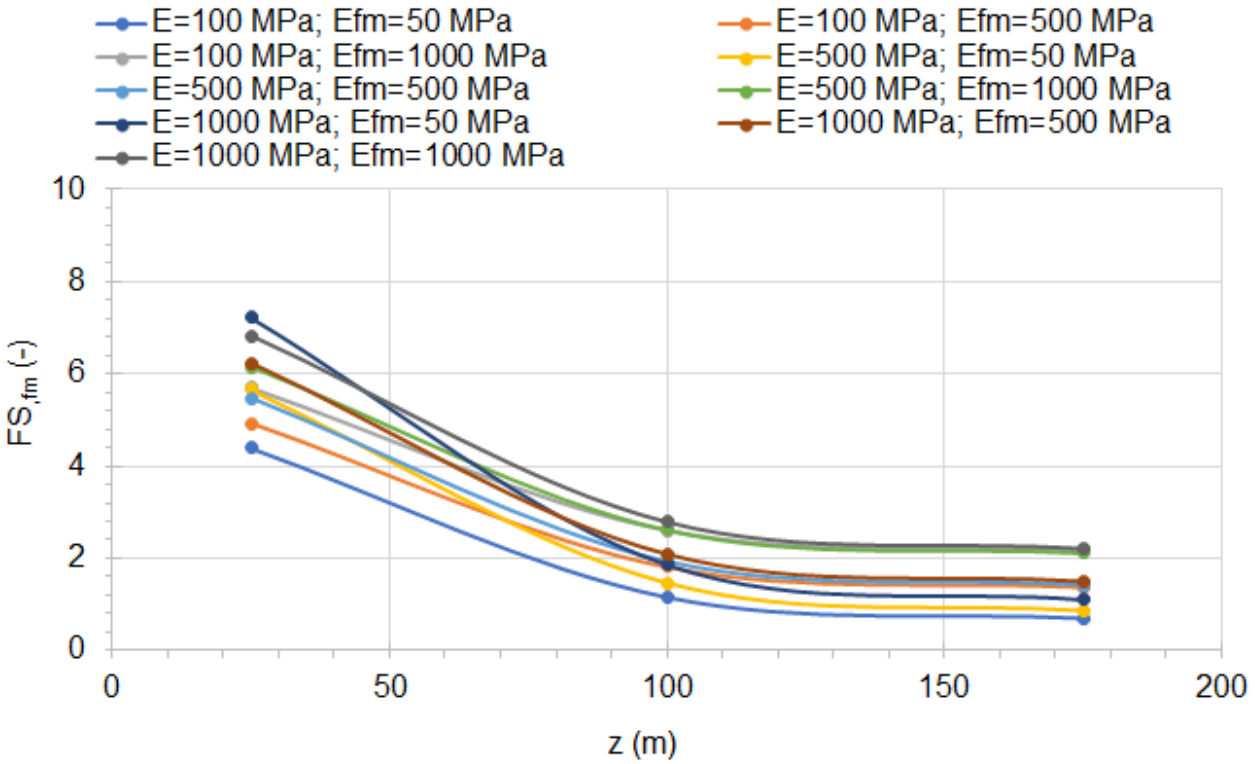

439

440 **Fig. 18. Safety factors in the filling material ($FS_{,fm}$) as the depth z of the tunnel varies,**
441 **for different values of the elastic modulus of the ground (E) and of the elastic modulus**
442 **of the filling material (E_{fm}). Case of a tunnel with radius R = 5 m.**

443

444 **Conclusions**

445 As the two-component material cures over time, the mechanical characteristics tend to vary
446 over time, until they stabilize after some time. In the study of the behavior of the support
447 system, it is of interest to evaluate the average elastic modulus, during the loading phase of
448 the support system. Several laboratory studies for the evaluation of the mechanical
449 characteristics of the two-component material have been developed and the results are
450 available in the scientific literature. In particular, a certain variability of the values is noted,
451 as a function not only of the different types of materials used, but also of the sample
452 preparation. Therefore, there is an uncertainty about the actual mechanical characteristics

of the filling material on site, during the construction of the tunnel and the installation of the support system.

In this work, an extensive parametric analysis was developed (243 cases) able of representing all possible cases of tunnels excavated using TBM machines in soils (from soft to stiff), of different diameters and depths. The study was carried out using two different analytical methods known in the literature: the convergence-confinement method (CCM) and the Einstein and Schwartz method. From them it is possible to determine the stress state induced in the concrete constituting the segmental lining.

From the results obtained, it is possible to detect how:

1. The K_0 coefficient (lateral earth pressure at rest in the ground) has a particular influence on the value of the maximum stresses reached in the concrete of the segmental lining: the further K_0 moves away from the unity, the greater the maximum stress in the concrete;
2. The stiffness of the ground (elastic modulus E) produces effects on the maximum stress in the concrete: the stress tends to increase as the elastic modulus decreases, in particular for E <500 MPa and for medium and high tunnel radii R (R ≥ 3.5 m);
3. The stiffness of the filling material (elastic modulus E_{fm}) produces effects on the maximum stress in the concrete especially when the elastic modulus E of the soil is high; however, no influence of the filling material on the segmental lining is noted when its elastic modulus E_{fm} is less than 500 MPa.
4. In general, the maximum stresses in concrete obviously tend to increase as the radius of the tunnel and its depth increase.

Then considering a failure criterion for the concrete, it was possible to determine the safety factor with regard to the possible failure of the segmental lining ($FS_{,sl}$). The obtained results were plotted according to all the analyzed parameters, constituting a useful design tool for sizing the support system in the presence of the filling material around the segmental lining.

In particular, the lowest safety factors are found for K_0 distant from the unity, for E_{fm} greater than 500 MPa and for lower elastic modules of the ground. There is no influence on $FS_{,sl}$ when E_{fm} ≥ 500 MPa. In general, the safety factors tend to decrease as the depth of the tunnel and its radius increase.

In the support system design phase, it must also be verified that the filling material does not fail in the gap between the external profile of the segmental lining and the tunnel wall. For this reason it is useful to analyze the trend of the safety factor of the filling material ($FS_{,fm}$) as the parameters considered in the study vary. The graphs show that the lowest values are obtained for high depths, soft soils and relatively low elastic modulus of the filling material.

In the design phase, therefore, it is possible to identify, also thanks to the procedure developed in this paper, what the mechanical characteristics of the filling material must be in order to guarantee adequate safety factors for the segmental lining and the filling material itself. In particular, it is useful to intervene on the stiffness characteristic of the material (E_{fm}) given its influence both on the maximum stress in the concrete and in the filling material itself. Furthermore, through a careful definition of the dosages, it is possible to reach a uniaxial compressive strength (UCS) of the filling material, such as to avoid its failure with all the consequences on the effective seal of the support system from the hydraulic point of view and on its durability.

Conflict of interests

Authors declare they have no conflict of interest.

The authors declare that no funds, grants, or other support were received during the preparation of this manuscript.

References

Amberg W, Lombardi G (1974) Une Méthode de Calcul Elastoplastique de l'Etat de Tension et de Déformation Autour d'une Cavité Souterraine. Proc. 3rd Int. Congr. Rock Mech., Denver, Vol. IIB, pp.1055-1069.

Beghoul M, Demagh R (2019) Slurry shield tunneling in soft ground. Comparison between field data and 3D numerical simulation. Studia Geotechnica et Mechanica, 41(3), 115–128.

BS (1983) 1881: Part 120 Method of determination of compressive strength of concrete cores. British Standards Institution.

Dai Z, Bai Y, Peng F, Liao S (2010) Study on mechanism of simultaneous backfilling grouting for shield tunnelling in soft soils. GeoShanghai Int. Conf. on Deep and Underground Excavations, ASCE, Reston, VA, 182–190.

Dias TGS, Bezuijen A (2015) TBM Pressure Models - Observations, Theory and Practice. 15th Pan-American Conference on Soil Mechanics and Geotechnical Engineering - Geotechnical Synergy in Buenos Aires 2015, 347–374, 2015. doi: 10.3233/978-1-61499-599-9-347.

Di Giulio A, Bavasso I, Di Felice M, Sebastiani D (2020) A preliminary study of the parameters influencing the performance of two-component backfill grout. Gallerie e Grandi Opere Sotterranee, 133, 11-17.

Do, NA, Dias D, Oreste P, Djeran-Maigre I (2013) 3D modelling for mechanized tunnelling in soft ground-influence of the constitutive model. American Journal of Applied Sciences, 10(8), 863–875.

Do, NA, Dias D, Oreste P, Djeran-Maigre I (2015) Behaviour of segmental tunnel linings under seismic loads studied with the hyperstatic reaction method. Soil Dyn Earthq Eng 79:108–117.

Einstein HH, Schwartz CW (1979) Simplified analysis for tunnel support. J Geotech Eng, 105, GT4:499-518.

Flores AQ (2015) Physical and mechanical behavior of a two component cement-based grout for mechanized tunneling application. MSc Thesis, Universidade Federal do Rio de Janeiro, Brazil.

Guan Z, Deng T, Wang G, Jiang Y (2015) Studies on the key parameters in segmental lining design. J Rock Mech Geotech Eng, 7(6): 674-683.

Kravitz B, Mooney M, Karlovsek J, Danielson I, Hedayat A (2019) Void detection in two-component annulus grout behind a pre-cast segmental tunnel liner using Ground Penetrating Radar. Tunn Undergr Space Technol 83:381-392. *https://doi.org/10.1016/j.tust.2018.09.032*.

Ochmański M, Modoni G, Bzówka J (2018) Automated numerical modelling for the control of EPB technology. Tunn Undergr Space Technol 75: 117–128. *https://doi.org/10.1016/j.tust.2018.02.006*.

Ochmański M, Modoni G, Spagnoli G (2021) Influence of the annulus grout on the soil-lining interaction for EBP tunneling. Geotechnical Aspects of Underground Construction in Soft Ground: Proceedings of the Tenth International Symposium on Geotechnical Aspects of Underground Construction in Soft Ground, IS-Cambridge 2022, Cambridge, United Kingdom, 27-29 June 2022, 350-356, DOI: *10.1201/9780429321559-45.*

Oggeri C, Oreste P, Spagnoli G (2021) The influence of the two-component grout on the behaviour of a segmental lining in tunnelling. Tunn Undergr Space Technol 109:103750, https://doi.org/10.1016/j.tust.2020.103750.

Oggeri C, Oreste P, Spagnoli G (2022) Creep behaviour of two-component grout and interaction with segmental lining in tunnelling. Tunn Undergr Space Technol 119:104216

Oh JY, Ziegler M (2014) Investigation on influence of tail void grouting on the surface settlements during shield tunneling using a stress-pore pressure coupled analysis. KSCE J Civ Eng 18(3):803-811. DOI: 10.1007/s12205-014-1383-8.

552 Oreste P (2003). Analysis of structural interaction in tunnels using the covergence–
553 confinement approach. Tunn Undergr Space Technol 18, 4:347-363.
554 Oreste P (2009). The convergence-confinement method: roles and limits in modern
555 geomechanical tunnel design. American Journal of Applied Sciences 6(4):757-771.

556 Oreste P, Sebastiani D, Spagnoli G, de Lillis A (2021) Analysis of the behavior of the two-
557 component grout around a tunnel segmental lining on the basis of experimental results and
558 analytical approaches, Transp. Geotech 29: 100570,
559 https://doi.org/10.1016/j.trgeo.2021.100570.
560 Panet M, Guenot A (1982) Analysis of convergence behind the face of a tunnel. Tunnelling
561 82, proceedings of the 3rd international symposium, Brighton, 7–11 June 1982, 197–204.

562 Peila D, Borio L, Pelizza S (2011) The behaviour of a two-component backfilling grout used
563 in a Tunnel-Boring Machine. Acta Geotech Slov 1:5–15.

564 Pelizza S, Peila. D, Sorge R, Cignitti F (2011) Back-fill grout with two component mix in EPB
565 tunneling to minimize surface settlements: Rome Metro - Line C case history. Proceedings
566 of Geotechnical Aspects of Underground Construction in Soft Ground. Viggiani. G. (ed.).
567 291-299. Taylor & Francis Group. London.
568 Rahmati, S, Chakeri H, Sharghi M, Dias D (2022) Experimental study of the mechanical
569 properties of two-component backfilling grout. Proc Inst Civ Eng: Ground Improv 175, 4:
570 277-289, *https://doi.org/10.1680/jgrim.20.00037*
571 Shah, R., Lavasan, A.A. , Peila. D., Todaro. C., Luciani. A. and Schanz, T. (2018). Numerical
572 study on backfilling the tail void using a two-component grout. J. Mater. Civ. Eng., 30(3):
573 04018003.
574 Sharghi M, Chakeri H, Afshin H, Ozcelik Y (2018) An experimental study of the performance
575 of two-component backfilling grout used behind the segmental lining of a Tunnel-Boring

576 Machine. J Test Eval 46,5: 2083–2099, https://doi.org/10.1520/JTE20160617. ISSN 0090-
577 3973
578 Spagnoli G, Oreste P, Bianco LL (2016) New equations for estimating radial loads on deep
579 shaft linings in weak rocks. Int J Geomech, 16(6):06016006
580 Talmon AM, Bezuijen A (2005) Grouting the tail void of bored tunnels: the role of hardening
581 and consolidation of grouts. Proceedings of the 5th International Symposium TC 28 -
582 Geotechnical Aspects of Underground Construction in Soft Ground, 125-130, Balkema,
583 Rotterdam.
584 Thewes M, Budach C (2009) Grouting of the annular gap in shield tunnelling-An important
585 factor for minimisation of settlements and production performance. Proceedings of the ITA-
586 AITES World Tunnel Congress 2009 “Safe Tunnelling for the City and Environment”. pp. 1–
587 9.
588 Todaro C, Bongiorno M, Carigi A, Martinelli D (2020) Short term strength behavior of two-
589 component backfilling in shield tunneling: comparison between standard penetrometer test
590 results and UCS. Geoingegneria Ambientale e Mineraria 57, 1:33-40.
591 Todaro C, Carigi A, Martinelli D, Peila D (2021) Study of the shear strength evolution over
592 time of two-component backfilling grout in shield tunnel. Case Studies in Construction
593 Materials 15, e00689, *https://doi.org/10.1016/j.cscm.2021.e00689*.
594 Todaro C, Martinelli D, Boscaro A, Carigi A, Saltarin S, Peila D (2022) Characteristics and
595 testing of two-component grout in tunnelling applications. Geomech Tunn 15, 1: 121-131,
596 *https://doi.org/10.1002/geot.202100019*.
597 Vlachopoulos N, Diederichs M.S. (2009) Improved longitudinal displacement profiles for
598 convergence confinement analysis of deep tunnels. Rock Mech Rock Eng, 42:131–146.
599 Zaheri M, Ranjbarnia M, Dias D, Oreste P (2020) Performance of segmental and shotcrete
600 linings in shallow tunnels crossing a transverse strike-slip faulting. Transp Geotech 23:
601 100333.